JACS
JOURNAL OF THE AMERICAN CHEMICAL SOCIETY

Communication

pubs.acs.org/JACS

Participation of Electron Transfer Process in Rate-Limiting Step of Aromatic Hydroxylation Reactions by Compound I Models of Heme Enzymes

Maaya Asaka and Hiroshi Fujii*

Department of Chemistry, Graduate School of Humanities and Sciences, Nara Women's University, Kitauoyanishi, Nara 630-8506, Japan

Supporting Information

ABSTRACT: Hydroxylation reactions of aromatic rings are key reactions in various biological and chemical processes. In spite of their significance, no consensus mechanism has been established. Here we performed Marcus plot analysis for aromatic hydroxylation reactions with oxoiron(IV) porphyrin π-cation radical complexes (compound I). Although many recent studies support the mechanism involving direct electrophilic attack of compound I, the slopes of the Marcus plots indicate a significant contribution of an electron transfer process in the rate-limiting step, leading us to propose a new reaction mechanism in which the electron transfer process between an aromatic compound and compound I is in equilibrium in a solvent cage and coupled with the subsequent bond formation process.

Hydroxylations of aromatic rings are important biological and chemical reactions and are catalyzed by various metalloenzymes and metal catalysts.[1−6] Among these reactions, the aromatic hydroxylation reactions catalyzed by cytochrome P450 have been studied for the past decades with relation to detoxification processes, biosynthesis, and carcinogenicity via DNA mutations.[1−4] Like most monooxygenation reactions by cytochrome P450, the aromatic hydroxylation reactions are mediated by oxoiron(IV) porphyrin π-cation radical species (compound I).[7] The mechanism of the aromatic hydroxylation reaction has been extensively investigated using liver microsomal fractions, isolated cytochrome P450, and its iron porphyrin model complexes, and several reaction mechanisms have been proposed (Scheme 1). Pathway A involves an initial electrophilic attack of compound I on an aromatic compound to form an arene oxide.[8,9] Pathway B is similar to pathway A, but a tetrahedral σ intermediate is formed via the electrophilic attack of compound I.[10−16] Pathway C involves an initial electron transfer to form an oxoiron(IV) porphyrin species (compound II) and an aromatic radical species followed by the bond formation to yield the tetrahedral σ intermediate.[17] Pathway D is analogous to the rebound mechanism proposed for alkane hydroxylation, in which abstraction of a hydrogen atom of an aromatic ring by compound I is followed by rebound of the hydroxyl group.[9] The meta-hydroxylation of chlorobenzene and biphenyl is inconsistent with the direct arene oxide formation (pathway A).[10] The mechanism involving hydrogen abstraction (pathway D) has been ruled

Scheme 1. Proposed Reaction Mechanisms for Aromatic Hydroxylation Reactions by Compound I

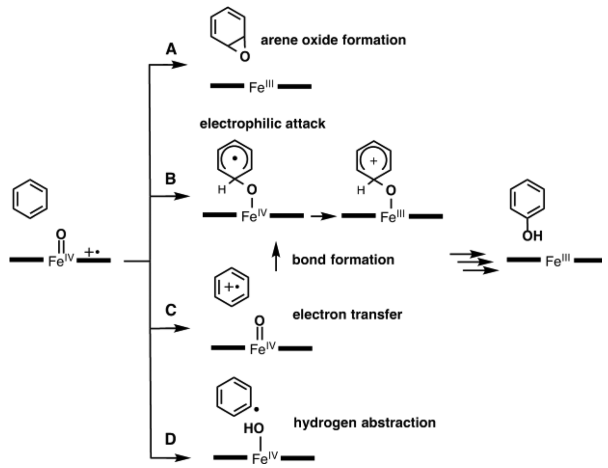

out by the experimental results of a small hydrogen/deuterium kinetic isotope effect (KIE) and the 1,2-hydride shift to a carbocationic center (NIH shift) in the aromatic hydroxylation. The formation of an aromatic cation radical species has been reported in the reaction of cytochrome P450 with 1,2,4,5-tetramethoxybenzene having a low oxidation potential, suggesting the initial electron transfer (pathway C).[17] However, theoretical calculations denied pathways C and D and rather supported the direct electrophilic attack mechanism shown in pathway B.[12−14] A recent kinetic study of synthetic compound I model complexes with benzene afforded a large negative Hammett ρ value, supporting pathway B.[15] While the mechanism of the aromatic hydroxylation reaction has been studied by many groups, there is no consensus mechanism that can explain all of the experimental results. In this paper, on the basis of Marcus plot analysis,[18] we propose a new mechanism by which all of the experimental results can be explained reasonably.

To construct the Marcus plot, we prepared compound I model complexes having different redox potentials, shown in Figure 1, and performed kinetic studies of the aromatic hydroxylation reactions with anisole, benzene, and naphthalene. The redox potentials of these compound I model complexes are

Received: March 29, 2016
Published: June 21, 2016

DOI: 10.1021/jacs.6b03223
J. Am. Chem. Soc. 2016, 138, 8048−8051

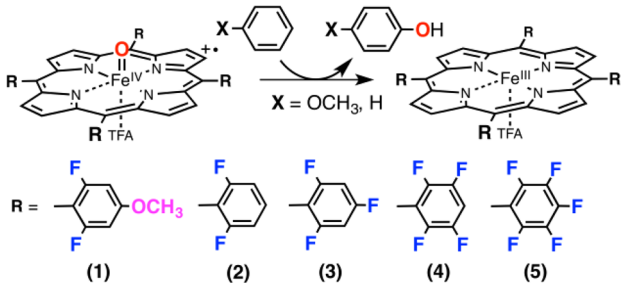

Figure 1. Structures of compound I model complexes used in this study.

modulated by the number of fluorine atoms in the *meso*-phenyl groups of the porphyrin ligand without changing the steric effect around the oxo ligand (Figure 1). The compound I model complexes of **1**−**5** were prepared by oxidation of the corresponding ferric trifluoroacetate (TFA) complexes with ozone gas, followed by removal of excess ozone gas with bubbling argon gas, in dichloromethane at −80 °C.[19] Figure 2

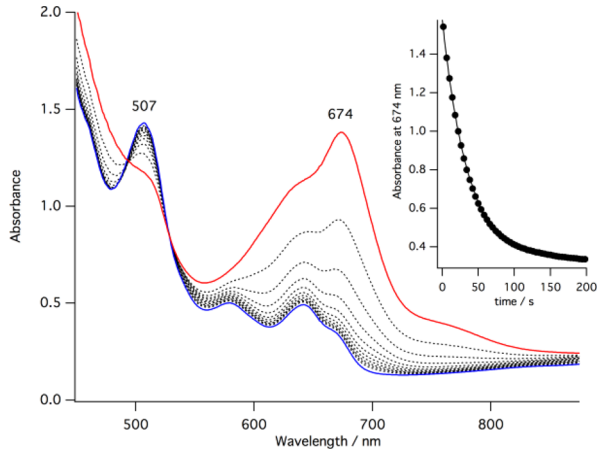

Figure 2. Absorption spectral changes for the reaction of compound I model complex of **1** with anisole. Red line: immediately after addition of anisole. Black dotted lines: absorption spectral changes at 4 s intervals. Blue line: the final spectrum of the reaction. Inset: Time course of the absorbance at 674 nm for the reaction. The solid line indicates simulation of the time course with a single-exponential function.

shows absorption spectral changes for the reaction of compound I model complex of **1** with anisole at −80 °C. The absorption spectrum of **1** changes to that of the ferric complex with clear isosbestic points. Similar absorption spectral changes with clear isosbestic points are observed for the reactions of the other compound I model complexes with anisole, benzene, and naphthalene (Figures S1−S3). The time courses of the absorbance for the reactions of the compound I model complexes with these aromatic compounds can be simulated with a single-exponential function, providing the second-order rate constants from the dependence on the concentration of the aromatic compound (Figures S4−S15). The reactions of compound I model complex of **5** with anisole and naphthalene were too fast for the reaction process to be followed with an absorption spectrometer, and the reaction of compound I model complex of **1** with benzene was too slow for the kinetic experiment to be carried out. The estimated second-order rate constants are listed in Table 1. The second-order rate constant increases with an increase in the number of fluorine atoms in the *meso*-phenyl groups (**1** < **2** < **3** < **4** < **5**), and an approximately 1000-fold difference between **1** and **4** for anisole and **2** and **5** for benzene was observed.

The KIE for the reaction of **2** with anisole was determined with deuterium labeled anisole-d_8 (Figure S16) and was found to be 0.92 ± 0.08. Similar KIE values were reported for benzene, toluene, and naphthalene in a previous paper.[15] The observed very small KIE values are consistent with electrophilic attack of the oxo ligand on the sp^2 carbon center of the aromatic compound in the rate-limiting step (pathway B) but are inconsistent with the hydrogen abstraction mechanism shown in pathway D.

Product analysis of these reactions under single-turnover conditions at −80 °C indicated the formation of 4-methoxyphenol (6−65%) from anisole, 1-naphthol (10%) and 1,4-naphthoquinone (5%) from naphthalene, and phenol (4%) and *p*-benzoquinone (2%) from benzene (Table S1). The reaction of benzene under catalytic conditions at −40 °C afforded *p*-benzoquinone (188%) as the major product (Table S1), as reported in previous studies.[15,17] The reaction of the ^{18}O-isotope-labeled compound I model complex of **4** with anisole under single-turnover conditions showed the incorporation of the ^{18}O atom (60%) into 4-methoxyphenol (Table S1). These results indicate that the compound I model complexes catalyze these aromatic hydroxylation reactions.

The redox potentials of compound I/compound II redox couples were determined from electrochemical measurements on compound II model complexes of **1**−**5** at low temperature. The compound II model complexes of **1**−**5** were prepared by ozone oxidation of ferric hydroxide complexes in acetonitrile at −40 °C. Quasi-reversible redox waves were observed in cyclic voltammograms (CVs) and differential pulse voltammograms (DPVs) of compound II model complexes of **1**−**5** (Figures S17 and S18). We previously reported that these redox couples are assignable to the compound I/compound II redox couples.[20] The half-wave potentials of the compound I/compound II redox couples, $E_{1/2}$(I/II), for **1**−**5** were determined and are listed in Table 1.

To investigate the electron transfer process in the aromatic hydroxylation reaction, we constructed plots of $(RT/F)\ \ln(k_2)$ versus $\Delta E_{1/2}$(I/II) for the present hydroxylation reactions

Table 1. Second-Order Rate Constants and Redox Potentials of 1−5

	1	2	3	4	5
k_2(anisole)/M^{-1} s^{-1}	(5.83 ± 0.13) × 10^{-1}	4.82 ± 0.26	(2.59 ± 0.11) × 10	(5.09 ± 0.38) × 10^2	nd
k_2(benzene)/M^{-1} s^{-1}	nd	(2.00 ± 0.20) × 10^{-4}	(9.24 ± 0.63) × 10^{-4}	(5.81 ± 0.12) × 10^{-2}	(2.42 ± 0.25) × 10^{-1}
k_2(naphthalene)/M^{-1} s^{-1}	1.04 ± 0.05	6.01 ± 0.13	(1.52 ± 0.05) × 10	(5.90 ± 0.30) × 10^2	nd
$E_{1/2}$(I/II)/V vs SCE	1.120	1.177	1.214	1.294	1.358
$\Delta G^{\ddagger}/\Delta G_{ET}$ (anisole)/kJ·mol^{-1}	47.5/62.7	44.0/57.2	41.3/53.7	36.6/45.9	nd
$\Delta G^{\ddagger}/\Delta G_{ET}$ (benzene)/kJ·mol^{-1}	nd	60.9/123.8	55.4/120.2	51.1/112.5	48.9/106.3

DOI: 10.1021/jacs.6b03223
J. Am. Chem. Soc. 2016, 138, 8048−8051

(Figure 3). The plots can be simulated well with linear functions with the slopes of 0.68 ± 0.07 for benzene, 0.65 ±

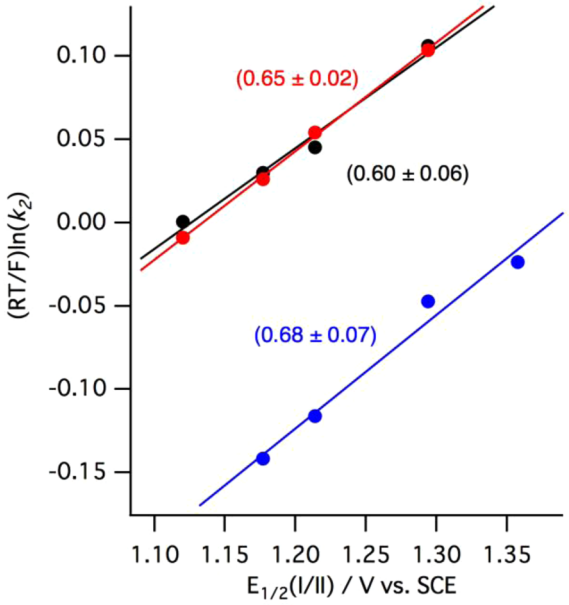

Figure 3. Plots of $(RT/F)\ \ln(k_2)$ vs $E_{1/2}$(I/II) for the reactions of compound I model complexes with anisole (red), benzene (blue), and naphthalene (black) at −80 °C. The numbers in the parentheses are the slopes of the fitted lines.

0.02 for anisole, and 0.60 ± 0.06 for naphthalene. According to the Marcus theory, a plot of $(RT/F)\ \ln(k_2)$ versus $\Delta E_{1/2}$(I/II) should be linear with a slope of 0.5 when the electron transfer is exergonic.[18] The observed slopes clearly indicate the involvement of an electron transfer process in the rate-limiting step.

The half-wave potentials of anisole (1.77 V) and benzene (2.46 V), $E_{1/2}$(Ar), are much higher than the $E_{1/2}$(I/II) values.[21,22] Thus, the processes of electron transfer from compound I model complexes of **1**−**5** to aromatic compounds are endergonic. The driving force for electron transfer, ΔG_{ET} (calculated from the relationship $\Delta G_{ET} = -nF\Delta E$, where $n = 1$ for a one-electron transfer process, F is Faraday's constant, and ΔE is electromotive force), is larger than the free energy of activation, $\Delta G^{\ddagger}$, of the aromatic hydroxylation reaction (estimated from the Eyring equation, $\Delta G^{\ddagger} = -RT\ \ln(hk_2/kT)$, where R is the gas constant, T is the absolute temperature, h is Planck's constant, k is Boltzmann's constant, and k_2 is the second-order reaction rate constant) (Table 1).[23] Therefore, a simple electron transfer reaction from the compound I model complex to the aromatic compound, shown in pathway C, is not involved in these aromatic hydroxylation reactions.

An analysis originally reported by Ram and Hupp[24] affords a reasonable explanation for the large slopes observed in Figure 3. This analysis has been applied to hydrogen atom transfer reactions, in which the electron transfer process is endergonic and coupled with the subsequent proton transfer process.[25−27] In these reactions, when the proton transfer process is much slower than the electron transfer process, the electron transfer process would be in equilibrium, and therefore, the slope of the plot should be 1.0. On the other hand, when the rates of the electron transfer and proton transfer are comparable and thereby coupled to each other, a value between 0.5 and 1.0 would be observed. The observed slopes between 0.5 and 1.0 in Figure 3 indicate that the electron transfer process must be coupled with the subsequent process. Since the proton is not transferred in the rate-limiting step of the hydroxylation reaction, as supported by the KIE values, we propose that the electron transfer process is coupled with the subsequent bond formation process (Scheme 2). In the initial stage of the

Scheme 2

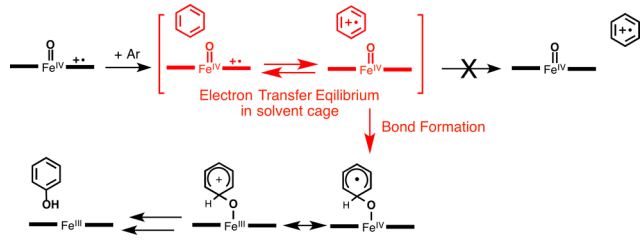

hydroxylation reaction, compound I makes a solvent-caged complex with the aromatic compound, and then the electron transfer occurs from the aromatic compound to compound I to form an aromatic π-cation radical and compound II in the solvent cage. The electron transfer process is in equilibrium in a solvent cage and coupled with the process of bond formation between the aromatic π-cation radical and the oxo ligand of compound II, resulting in a tetrahedral σ intermediate as proposed in pathway B. This mechanism is different from the mechanism shown in pathway C and is feasible because the electron-transferred state in the solvent cage is an intermediate of the endergonic electron transfer process and much more stable than the completely electron-transferred state proposed in pathway C.

This mechanism can reasonably explain previous experimental results because it involves the electron-transferred complex and the tetrahedral σ intermediate in one rate-limiting step. The observation of the aromatic π-cation radical species of 1,2,4,5-tetramethoxybenzene is quite reasonable because such a radical species can be easily liberated from the solvent cage when the electron transfer process is exergonic, i.e., when the redox potential of aromatic compound is lower than that of compound I.[17] The NIH shift and regioselectivity can be also explained by the participation of the tetrahedral σ intermediate in this mechanism.[9,10] This mechanism is also supported by the results of theoretical calculations, which predicted that the rate constant for the aromatic hydroxylation should be correlated with the ionization potential of the aromatic compound and the electron affinity of the compound I species.[14,28]

In summary, we carried out Marcus plot analysis of aromatic hydroxylation reactions by compound I model complexes. The slopes of the Marcus plots indicate a significant contribution of an electron transfer process in the rate-limiting step and allowed us to propose a new reaction mechanism in which the electron transfer between an aromatic compound and compound I is in equilibrium in a solvent cage and coupled with the subsequent bond formation process.

■ ASSOCIATED CONTENT

Supporting Information

The Supporting Information is available free of charge on the ACS Publications website at DOI: 10.1021/jacs.6b03223.

Experimental details, Table S1, and Figures S1−S18 (PDF)

DOI: 10.1021/jacs.6b03223
J. Am. Chem. Soc. 2016, 138, 8048−8051

AUTHOR INFORMATION

Corresponding Author

*fujii@cc.nara-wu.ac.jp

Notes

The authors declare no competing financial interest.

ACKNOWLEDGMENTS

This work was supported by a Grant-in-Aid for Scientific Research (25288032) from JSPS.

REFERENCES

(1) Fitzpatrick, P. F. *Biochemistry* **2003**, *42*, 14083−14091.
(2) Oritz de Montellano, P. R. In *Cytochrome P450: Structure, Mechanism, and Biochemistry*, 2nd ed.; Oritz de Montellano, P. R., Ed.; Plenum Press: New York, 1995; Chapter 8, pp 245−303.
(3) Guengerich, F. P. *Chem. Res. Toxicol.* **2001**, *14*, 611−650.
(4) Ullrich, R.; Hofrichter, M. *Cell. Mol. Life Sci.* **2007**, *64*, 271−293.
(5) Shoji, O.; Kunimatsu, T.; Kawakami, N.; Watanabe, Y. *Angew. Chem., Int. Ed.* **2013**, *52*, 6606−6610.
(6) Schmidt, R. *Appl. Catal., A* **2005**, *280*, 89−103.
(7) Rittle, J.; Green, M. T. *Science* **2010**, *330*, 933−937.
(8) Jerina, D. M.; Daly, J. W. *Science* **1974**, *185*, 573−582.
(9) Tomaszewski, J. E.; Jerina, D. M.; Daly, J. W. *Biochemistry* **1975**, *14*, 2024−2031.
(10) Korzekwa, K. R.; Swinney, D. C.; Trager, W. F. *Biochemistry* **1989**, *28*, 9019−9027.
(11) Vannelli, T.; Hooper, A. B. *Biochemistry* **1995**, *34*, 11743−11749.
(12) de Visser, S. P.; Shaik, S. *J. Am. Chem. Soc.* **2003**, *125*, 7413−7424.
(13) Bathelt, C. M.; Ridder, L.; Mulholland, A. J.; Harvey, J. N. *J. Am. Chem. Soc.* **2003**, *125*, 15004−15005.
(14) Shaik, S.; Milko, P.; Schyman, P.; Usharani, D.; Chen, H. *J. Chem. Theory Comput.* **2011**, *7*, 327−339.
(15) Kang, M.-J.; Song, W. J.; Han, A.-R.; Choi, Y. S.; Jang, H. G.; Nam, W. *J. Org. Chem.* **2007**, *72*, 6301−6304.
(16) Burka, L. T.; Plucinski, T. M.; Macdonald, T. L. *Proc. Natl. Acad. Sci. U. S. A.* **1983**, *80*, 6680−6684.
(17) Sato, H.; Guengerich, F. P. *J. Am. Chem. Soc.* **2000**, *122*, 8099−8100.
(18) Marcus, R. A.; Sutin, N. *Biochim. Biophys. Acta, Rev. Bioenerg.* **1985**, *811*, 265−322.
(19) Cong, Z.; Kurahashi, T.; Fujii, H. *J. Am. Chem. Soc.* **2012**, *134*, 4469−4472.
(20) Takahashi, A.; Kurahashi, T.; Fujii, H. *Inorg. Chem.* **2011**, *50*, 6922−6928.
(21) Merkel, P. B.; Luo, P.; Dinnocenzo, J. P.; Farid, S. *J. Org. Chem.* **2009**, *74*, 5163−5173.
(22) Luo, P.; Feinberg, A. M.; Guirado, G.; Farid, S.; Dinnocenzo, J. P. *J. Org. Chem.* **2014**, *79*, 9297−9304.
(23) Eyring, H. *J. Chem. Phys.* **1935**, *3*, 107−115.
(24) Ram, M. S.; Hupp, J. T. *J. Phys. Chem.* **1990**, *94*, 2378−2380.
(25) Weatherly, S. C.; Yang, I. V.; Thorp, H. H. *J. Am. Chem. Soc.* **2001**, *123*, 1236−1237.
(26) Osako, T.; Ohkubo, K.; Taki, M.; Tachi, Y.; Fukuzumi, S.; Itoh, S. *J. Am. Chem. Soc.* **2003**, *125*, 11027−11033.
(27) Goto, Y.; Matsui, T.; Ozaki, S.-I.; Watanabe, Y.; Fukuzumi, S. *J. Am. Chem. Soc.* **1999**, *121*, 9497−9502.
(28) Kumar, D.; Sastry, G. N.; de Visser, S. P. *J. Phys. Chem. B* **2012**, *116*, 718−730.

DOI: 10.1021/jacs.6b03223
J. Am. Chem. Soc. 2016, 138, 8048−8051